

ACCEPTED MANUSCRIPT • OPEN ACCESS

## Radiocarbon as a tracer of the fossil fraction of regional carbon monoxide emissions

To cite this article before publication: Liam Blyth *et al* 2024 *Environ. Res. Lett.* in press <https://doi.org/10.1088/1748-9326/ad8248>

### Manuscript version: Accepted Manuscript

Accepted Manuscript is “the version of the article accepted for publication including all changes made as a result of the peer review process, and which may also include the addition to the article by IOP Publishing of a header, an article ID, a cover sheet and/or an ‘Accepted Manuscript’ watermark, but excluding any other editing, typesetting or other changes made by IOP Publishing and/or its licensors”

This Accepted Manuscript is © 2024 The Author(s). Published by IOP Publishing Ltd.



As the Version of Record of this article is going to be / has been published on a gold open access basis under a CC BY 4.0 licence, this Accepted Manuscript is available for reuse under a CC BY 4.0 licence immediately.

Everyone is permitted to use all or part of the original content in this article, provided that they adhere to all the terms of the licence <https://creativecommons.org/licenses/by/4.0>

Although reasonable endeavours have been taken to obtain all necessary permissions from third parties to include their copyrighted content within this article, their full citation and copyright line may not be present in this Accepted Manuscript version. Before using any content from this article, please refer to the Version of Record on IOPscience once published for full citation and copyright details, as permissions may be required. All third party content is fully copyright protected and is not published on a gold open access basis under a CC BY licence, unless that is specifically stated in the figure caption in the Version of Record.

View the [article online](#) for updates and enhancements.

# Radiocarbon as a Tracer of the Fossil Fraction of Regional Carbon Monoxide Emissions

Liam Blyth<sup>1,4</sup>, Heather Graven<sup>1</sup>, Alistair J Manning<sup>2</sup>, Pete Levy<sup>3</sup>

<sup>1</sup> Department of Physics, Imperial College London, London, SW7 2AZ, UK

<sup>2</sup> UK Met Office, Exeter, EX1 3PB, UK

<sup>3</sup> Centre for Ecology and Hydrology, Bush Estate, Penicuik, Midlothian EH26 0QB, UK

<sup>4</sup> Science and Solutions for a Changing Planet DTP, Imperial College London, London SW7 2BX, UK

Corresponding Author: [liam.blyth20@imperial.ac.uk](mailto:liam.blyth20@imperial.ac.uk)

## Abstract.

Carbon monoxide (CO) is an atmospheric pollutant with a positive net warming effect on the climate. The magnitude of CO sources and the fraction of fossil vs biogenic sources are still uncertain and vary across emissions inventories. Measurements of radiocarbon ( $^{14}\text{C}$ ) in CO could potentially be used to investigate the sources of CO on a regional scale because fossil sources lack  $^{14}\text{C}$  and reduce the  $^{14}\text{C}/\text{C}$  ratio ( $\Delta^{14}\text{C}$ ) of atmospheric CO more than biogenic sources. We use regional Lagrangian model simulations to investigate the utility of  $\Delta^{14}\text{C}$  measurements for estimating the fossil fraction of CO emissions and evaluating bottom-up emissions estimates (United Kingdom Greenhouse Gas, UKGHG, and TNO Copernicus Atmosphere Monitoring Service, TNO) in London, UK. Due to the high  $\Delta^{14}\text{C}$  in atmospheric CO from cosmogenic production, both fossil and biogenic CO emissions cause large reductions in  $\Delta^{14}\text{C}$  regionally, with larger reductions for fossil than biogenic CO per ppb added. There is a strong seasonal variation in  $\Delta^{14}\text{C}$  in background air and in the sensitivity of  $\Delta^{14}\text{C}$  to fossil and biogenic emissions of CO. In the UK, the CO emissions estimate from TNO has a higher fraction from fossil fuels than UKGHG (72% vs 67%). This results in larger simulated decreases in  $\Delta^{14}\text{C}$  per ppb CO for TNO emissions. The simulated differences between UKGHG and TNO are likely to be easily detectable by current measurement precision, suggesting that  $\Delta^{14}\text{C}$  measurements could be an effective tool to understand regional CO sources and assess bottom-up emissions estimates.

Submitted to: *Environ. Res. Lett.*

## *Radiocarbon as a Tracer of the Fossil Fraction of Regional Carbon Monoxide Emissions* 2

### **1. Introduction**

Carbon monoxide (CO) is a trace atmospheric gas which negatively impacts upon human health and indirectly contributes to climate change through its role in atmospheric chemistry. Removal of atmospheric CO is dominated by reaction with the hydroxyl radical (OH). CO has an atmospheric lifetime of  $\approx 1$ -2 months, although this varies in different parts of the atmosphere (Holloway et al., 2000). Although the direct radiative forcing effect of CO is negligible (Sinha et al., 1996), it accounts for 40% of the removal of OH, which impacts other species removed by OH (Lelieveld et al., 2016). Since OH is a sink for methane, an increase in CO concentration leads to a longer atmospheric lifetime for methane, increasing its forcing effect. This radiative effect of CO was estimated to be  $\approx 0.2 \text{ W}^{-2}$  as calculated in the 5<sup>th</sup> IPCC assessment in 2013 (Shindell et al., 2013).

Over the last 100 years, industrialisation led to a rise in CO emissions due to the incomplete combustion of fossil fuels and biomass, as well as an increase in chemical sources from oxidation of CH<sub>4</sub> (Duncan et al., 2007). Some economies have regulated emissions in recent decades for health reasons. To reduce emissions, these countries introduced catalytic converters in cars and shifted from coal and wood-powered heating to gas-fired boilers. These trends caused CO emissions to first increase in Europe and North America in the 20th century, then decline in the 21st century (Hoesly et al., 2018). In these regions, a clear downward trend in atmospheric CO concentrations has been observed since the late 1990s, with a substantial decrease in the most extreme high CO events (Figure 1) (Elguindi et al., 2020; Lowry et al., 2016). Along with a decrease in emissions, there has been a decrease in the fossil fraction of emissions as fossil fuel sources of CO have been mitigated more than biogenic sources. While the decrease in CO emissions in highly developed countries has stalled in recent years as many of the largest systematic and technological changes have already occurred, more work could still be done to further eliminate the remaining CO sources.

In regions that are in the process of industrialisation, such as in Asia and Africa, CO emissions and regional CO concentrations have risen over the past few decades and may continue to rise (Figure 1). Observed CO concentrations sometimes conflict with inversion techniques using bottom-up emissions estimates, which may also show strong differences between different estimates (Figure 1b), indicating that bottom-up approaches may not sufficiently quantify CO emissions. For example, observations by Zheng et al. (2018) indicated that emissions from East China over 2005-2016 decreased by  $\approx 2 \text{ \% yr}^{-1}$ , in contrast to the increasing trends in emissions estimated by global inventories. This suggests that emissions controls may not be properly accounted for in bottom-up approaches.

Here, we explore how CO source attribution could be possible using <sup>14</sup>C, a radioactive isotope of carbon produced naturally in the atmosphere. The half-life of <sup>14</sup>C (5700 years) is significantly less than the age of fossil fuel sources (coal, gas). As a result, CO produced from fossil fuel burning will be devoid of <sup>14</sup>CO, as the <sup>14</sup>C that was present when the fuel source formed has decayed away. In contrast, CO produced from biogenic sources will have

### Radiocarbon as a Tracer of the Fossil Fraction of Regional Carbon Monoxide Emissions 3

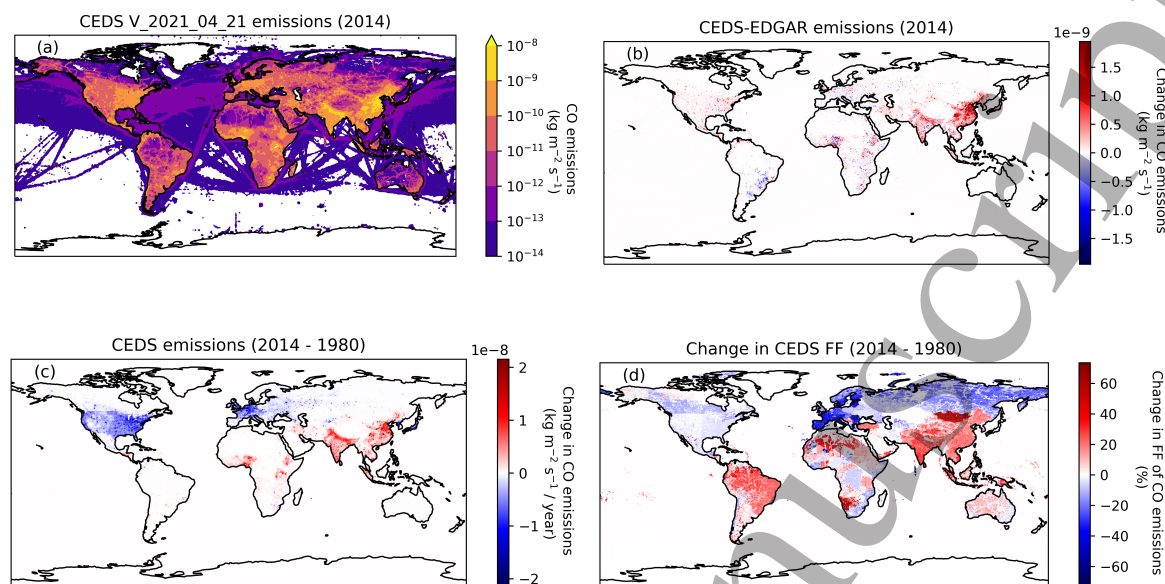


Figure 1: (a) CO emissions in 2014 from CEDS V\_2021\_04\_21 (henceforth known as CEDS) (Hoesly et al., 2018), (b) difference between CO emissions in CEDS and EDGAR version 6.1 in 2014 (c) difference in CO emissions in CEDS between 1980 and 2014 (d) difference in fossil fraction of CO emissions in CEDS between 1980 and 2014.

$^{14}\text{C}/\text{C}$  ( $\Delta^{14}\text{C}$ ,  $\Delta$  including correction for mass dependent fractionation as defined in Stuiver et al. (1977)) ratios similar to atmospheric  $\text{CO}_2$ .

$\Delta^{14}\text{C}$  measurements have been widely used to partition fossil fuel and biogenic sources of  $\text{CO}_2$  (Graven et al., 2018) and aerosols (Al-Naiema et al., 2018), but few previous studies have applied  $^{14}\text{CO}$  measurements to examine regional CO sources (Klouda et al., 1986; Moriizumi et al., 2004). Klouda et al. (1995) used this method in Albuquerque, USA in the winter of 1989/90. They found that motor vehicles dominated emissions, but residential wood combustion increased in the winter. Similarly, Sakugawa et al. (1997) conducted  $^{14}\text{CO}$  measurements in Los Angeles, USA, and found that CO measured was predominantly of motor vehicle origin but that wood-burning was significant in winter.

Other measurements of  $^{14}\text{C}$  in CO have been made to study CO loss by atmospheric OH rather than CO sources, and have typically been reported as molar density in units of molecules  $\text{cm}^{-3}$  rather than  $\Delta^{14}\text{C}$  (Jöckel et al., 2002a). Compared to  $\text{CO}_2$  and aerosols,  $\Delta^{14}\text{C}$  of CO in background air is much higher (Brenninkmeijer et al., 2022). Background values for  $\Delta^{14}\text{C}$  vary significantly over the globe because the main source of  $^{14}\text{CO}$  from cosmogenic production is focused in the high latitude upper troposphere and stratosphere (Poluianov et al., 2016). This causes high  $\Delta^{14}\text{C}$  in CO at surface levels at high latitudes, which varies seasonally due to the seasonal variation in stratosphere-troposphere exchange (Quay et al., 2000). Cosmogenic  $^{14}\text{CO}$  production is modulated by the solar cycle, so background  $\Delta^{14}\text{CO}$  also varies with solar

## Radiocarbon as a Tracer of the Fossil Fraction of Regional Carbon Monoxide Emissions 4

activity. The high background  $\Delta^{14}\text{CO}$  (2000 - 6000 ‰ estimated at Mace Head, Ireland) means that fossil (-1000 ‰) and biogenic (10-115 ‰ estimated for 2018) CO sources have a large difference in  $\Delta^{14}\text{C}$  signature from background  $\Delta^{14}\text{CO}$ , such that  $\Delta^{14}\text{CO}$  will be highly sensitive to regional CO emissions.

Here we present the first simulations of  $\Delta^{14}\text{CO}$  at a regional scale and use them to investigate the ability of  $\Delta^{14}\text{CO}$  measurements to quantify the fossil fraction of CO emissions on regional scales. We use the Met Office's Numerical Atmospheric-dispersion Modelling Environment (NAME) to simulate CO and  $\Delta^{14}\text{CO}$  at Imperial College London. We focus on Imperial College London (Saboya et al., 2022) where we currently conduct atmospheric measurements, including CO concentrations, and where we plan to measure  $\Delta^{14}\text{C}$  of CO in the future. From simulations based on different CO inventories and an idealised scenario, we simulate the effect of differences in the fossil fraction of CO emissions on  $\Delta^{14}\text{CO}$  in London.

## 2. Methods

This section lays out the approach for simulating the CO concentration and  $\Delta^{14}\text{CO}$  at Imperial College London for every hour in 2018. It will require an estimation of background CO and  $\Delta^{14}\text{CO}$ , as well as an understanding of fuel sources and fossil fraction of different sectors in the emissions schemes being tested.

### 2.1. Mass-Balance Approach

This section lays out the mass balance approach used to simulate CO and  $\Delta^{14}\text{C}$ . The mass-balance equation governing CO is:

$$C_m = C_{bg} + \sum_i C_i \quad (1)$$

where  $C_m$  represents the CO concentration simulated at our site of interest (Imperial College London),  $C_{bg}$  is the CO concentration at a background site (here, Mace Head, Ireland), and  $C_i$  is the simulated CO enhancement caused by emissions from sector  $i$ . Following previous studies of regional CO sources using Lagrangian models (Andersen et al., 2024; Ding et al., 2013), we assume that the effects of photochemical sources and sinks are negligible due to the short timescales (days) of air transport between background areas represented by Mace Head and the observation site in London.

The mass-balance equation governing  $^{14}\text{CO}$  is:

$$\Delta_m C_m = \Delta_{bg} C_{bg} + \sum_i \Delta_i C_i \quad (2)$$

Here, the additional terms  $\Delta_m$ ,  $\Delta_{bg}$ , and  $\Delta_i$  represent the  $\Delta^{14}\text{C}$  of CO at our site of interest, at the background site, and in emissions from sector  $i$ , respectively. Compared to prior work

## Radiocarbon as a Tracer of the Fossil Fraction of Regional Carbon Monoxide Emissions 5

with CO<sub>2</sub> and CH<sub>4</sub> where <sup>14</sup>C emissions from nuclear power plants have to be considered, it is unlikely that conditions amenable to the production of <sup>14</sup>CO are present in nuclear power plants and there are no indications of in-situ <sup>14</sup>CO production (Brenninkmeijer et al., 2022; Kunz, 1985). As with the CO mass balance, we assume photochemical sources and sinks have negligible effects on Δ<sub>m</sub> for the short timescales of transport between background areas and London.

### 2.2. Background CO and Δ<sup>14</sup>C

Very few <sup>14</sup>CO measurements are available for the last decade, so we construct an estimate of background Δ<sup>14</sup>C at Mace Head (53.3°N, 9.9°W) in 2018 using historical data (Derwent et al., 2020). For CO concentration, we use recent NOAA flask measurements at Mace Head, Ireland, for 2018. We find the monthly average CO mixing ratio and apply a sine function to calculate an estimated CO background for our simulations.

For <sup>14</sup>CO concentration, the background is estimated from measurements of <sup>14</sup>CO in Washington state, USA between 1991 and 1997 (Quay et al., 2000). The measurement station in Washington State shares similarities with Mace Head, as it is on the west coast of a continent and receives predominantly clean air from over the ocean. It is also at a similar latitude as Mace Head (supplementary Figure S1), meaning that background <sup>14</sup>CO values are expected to be similar. Since the cosmogenic <sup>14</sup>CO production is influenced by the solar cycle, a normalisation factor is applied to this estimate to transform into 2018 equivalent values. Average global production of <sup>14</sup>CO in 2018 was 1.964 molecules cm<sup>-3</sup>, higher than the average between 1991 and 1997 (1.605 molecules cm<sup>-3</sup>; calculated using the methodology presented in Poluianov et al. (2016)).

Firstly, all measurements from 1991 and 1997 are normalised to the production in 2018 using the following equation

$$C_{i,2018} = C_{i,t} * \frac{q_{2018}}{q_t} \quad (3)$$

Where C<sub>i,t</sub> is the concentration in a given year, t, in a given month, i. q<sub>2018</sub> is the estimated global production in 2018 (1.964 molecules cm<sup>-3</sup>), q<sub>i</sub> is the estimated global production in the year, t, and C<sub>2018,t</sub> is the normalised concentration, and so is C<sub>i,t</sub> normalised to 2018. This follows a similar process as Jöckel et al. (2002b), although we effectively normalise to an average solar production, and then ‘unnormalise’ to the solar production in 2018. We then calculate the average <sup>14</sup>CO for each month of 2018 and fit a sine function to generate our expected background. By combining our estimated CO and <sup>14</sup>CO we estimate Δ<sup>14</sup>C at Mace Head with the assumption of δ<sup>13</sup>C = -27.5‰ (Dasari et al., 2021).

## Radiocarbon as a Tracer of the Fossil Fraction of Regional Carbon Monoxide Emissions 16

### 2.3. Regional Anthropogenic Sources

We use two different anthropogenic emissions estimates to simulate CO and  $\Delta^{14}\text{C}$  at Imperial College London. These are the UK National Atmospheric Emissions Inventory with United Kingdom GHG time variability applied (UKGHG) and the TNO Copernicus Atmosphere Monitoring Service v5.3 (TNO) emissions inventory. They are similar in total UK CO emissions (1875 kilotonnes vs 1979 kilotonnes in 2018), however, the fuel source allocations and fossil fraction (FF, 67% vs 72%) vary (Table 1).

Emissions Scheme	Total UK emissions (ktonnes)	UK Fossil Fraction (%)
UKGHG	1875	67
TNO	1979	72
UKGHG_NT	1069	50

Table 1: Estimates of UK emissions and calculated fossil fraction for different emissions schemes using UKGHG, TNO and our constructed UKGHG\_NT.

UKGHG emissions are a UK-specific emissions estimates only covering the UK geographical area, whereas TNO emissions span Europe. For UKGHG simulations, the UKGHG's UK emissions have been nested in the TNO emissions for Europe.

We also consider a scenario (UKGHG\_NT) in which the transport sector does not emit CO, which simulates the changes expected from a full transition to electric vehicles. We specify the emissions in this scenario by taking the UKGHG emissions embedded within TNO and removing all transport emissions.

Sector	$\Delta^{14}\text{C}$ (‰)	Fossil Fraction (%)	UKGHG (%)	TNO(‰)
Energy Production	-770	79	15.5	22.4
Domestic Combustion	-350	41	37.5	31.1
Industrial Combustion	-790	81	3.5	1.1
Industrial Processes	-1000	0	0	0
Offshore	-1000	0	0	0
Solvent	-20	12	0	0
Other Transport	-950	96	23.7	24.8
Road Transport	-950	96	14.1	17.1
Waste	-465	52	0.9	0.6
Nature	30	7	4.9	2.1

Table 2: Values of  $\Delta^{14}\text{C}$  and fossil fraction used in the calculations and the fraction of UK emissions assigned to different sectors in the two schemes.

To estimate the  $\Delta^{14}\text{C}$  of each emission sector, we must first estimate  $\Delta^{14}\text{C}$  for each fuel source.

## *Radiocarbon as a Tracer of the Fossil Fraction of Regional Carbon Monoxide Emissions* 7

The UKGHG and TNO use the Selected Nomenclature for Air Pollution (SNAP) sectors for emissions maps, but contain no information on the fuel sources used; therefore, we use the fuel sources given for each sector in the National Atmospheric Emissions Inventory (NAEI) data for annual total emissions, which use Nomenclature for Reporting (NFR) sectors. For fossil fuels,  $\Delta^{14}\text{C}$  is  $-1000\text{‰}$ . For biogenic sources, the age of the biomass burned must be considered. We use a simple one-box model with a specified turnover time together with the atmospheric history of  $\Delta^{14}\text{C}$  in the Northern Hemisphere (Graven et al., 2017). For older carbon sources, such as wood, the turnover time was assumed to be 50 years (personal correspondence with Forestry England), while for younger carbon sources, such as grasses, the turnover time was assumed to be 1 year, giving  $\Delta^{14}\text{C}$  values of  $115\text{‰}$  and  $10\text{‰}$  in 2018, respectively. These values will be used for both natural and anthropogenic biomass burning. We map each NFR sector to a SNAP sector (supplementary Table S1), such that we have the proportion of emissions in each SNAP sector derived from each fuel source (supplementary Table S3). The  $\Delta^{14}\text{C}$  for each SNAP sector is found by taking a weighted average of  $^{14}\text{C}$  for each fuel source within that sector, weighting by CO emissions (Table 2)

TNO include time variations that vary by sector (Guevara et al., 2021), and UKGHG emissions are calculated by adding time variability to the otherwise temporally static NAEI (<https://github.com/NERC-CEH/ukghg>). The two main emissions sectors for CO are domestic combustion and transport emissions, and the yearly and daily/weekly variability in these two sectors can be seen in Figure 2. Domestic combustion emissions are higher in the winter due to domestic heating. The UKGHG time variation is driven by activity and has a smooth variation throughout the year, whereas TNO variation is driven by the observed temperature and therefore has more irregular variation. Domestic combustion also shows a daily cycle, with a peak of emissions both early in the morning (10 am) and later in the evening (6 pm), with a slight decrease in the daytime (Figure 2c). There is little yearly variability in traffic emissions (Figure 2b), however, there is a significant daily cycle, with clear peaks in the morning and evening rush hours, and smaller transport emissions on the weekend.

### *2.4. NAME Footprints*

NAME was used to simulate CO at Imperial College London ( $\approx 26\text{m a.g.l.}$ ;  $51.4999^\circ\text{N}$ ,  $0.1749^\circ\text{W}$ ; Saboya et al. (2022)). NAME is a Lagrangian particle dispersion model driven by meteorological fields from a numerical weather prediction model, the Met-Office Unified Model (UM). Within the UK, UM resolution is at 1.5 km, outside it is 12 km. In the model, particles move in a three-dimensional grid with transport driven by the UM. There is also a random walk element to simulate the atmosphere's turbulence. No chemical production or destruction of CO was included.

The NAME model was run in backwards mode for a total of 30 days over the domain  $97.9^\circ\text{W}$  -  $39.38^\circ\text{E}$ , and  $10.73^\circ\text{N}$  -  $79.06^\circ\text{N}$  and footprints providing the sensitivity of an observation to emissions between 0 m and 40m (surface) were calculated with a resolution of  $0.356^\circ \times 0.234^\circ$ . Footprints were calculated with hourly resolution for the first 24 hours and the remaining



## Radiocarbon as a Tracer of the Fossil Fraction of Regional Carbon Monoxide Emissions 8

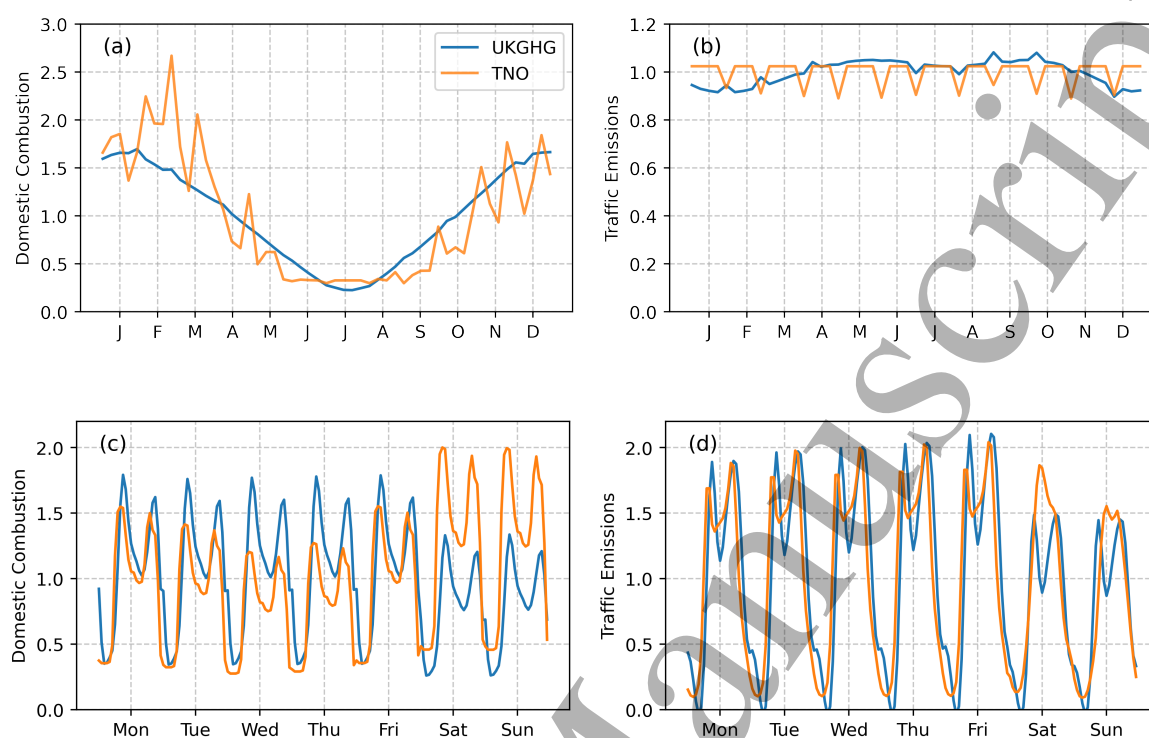


Figure 2: The normalised variability for the two main emissions sectors on different temporal scales for both UKGHG (blue) and TNO (orange) emissions in 2018. The yearly variation for domestic combustion in a), and the yearly variation for traffic emissions in b) shown as weekly averages. The weekly variation for domestic combustion can be seen in c), and the weekly variation for traffic is seen in d). In TNO, domestic combustion is calculated using atmospheric temperatures so there is no 'standard week'. Here, the first week of January was used.

29 days were time-integrated. Footprints from the first 24 hours with hourly resolution were multiplied by hourly emissions from UKGHG or TNO. The integrated footprint for the remaining 29 days enhancement was multiplied by the mean emissions for the month. These were then summed to produce the total simulated CO. Simulations were conducted for each emission sector and each hour in 2018.

### 3. Results

Simulated CO enhancements range from 2 to 225 ppb (daily 12:00-17:00 averages) and show a strong seasonality, with larger enhancements in winter (Figure 3a) that arise for two reasons. First, there are generally lower boundary heights in winter than summer, so the air is not mixed as extensively. Since London is the largest polluter in the area, the emissions from London are more confined in the local area, leading to greater CO enhancements. Second, CO emissions are higher in winter due to the increased combustion associated with domestic heating (Figure

## Radiocarbon as a Tracer of the Fossil Fraction of Regional Carbon Monoxide Emissions <sup>9</sup>

2). These simulations match previous measurements in and around London which also show a strong seasonality (Hernández-Paniagua et al., 2018).

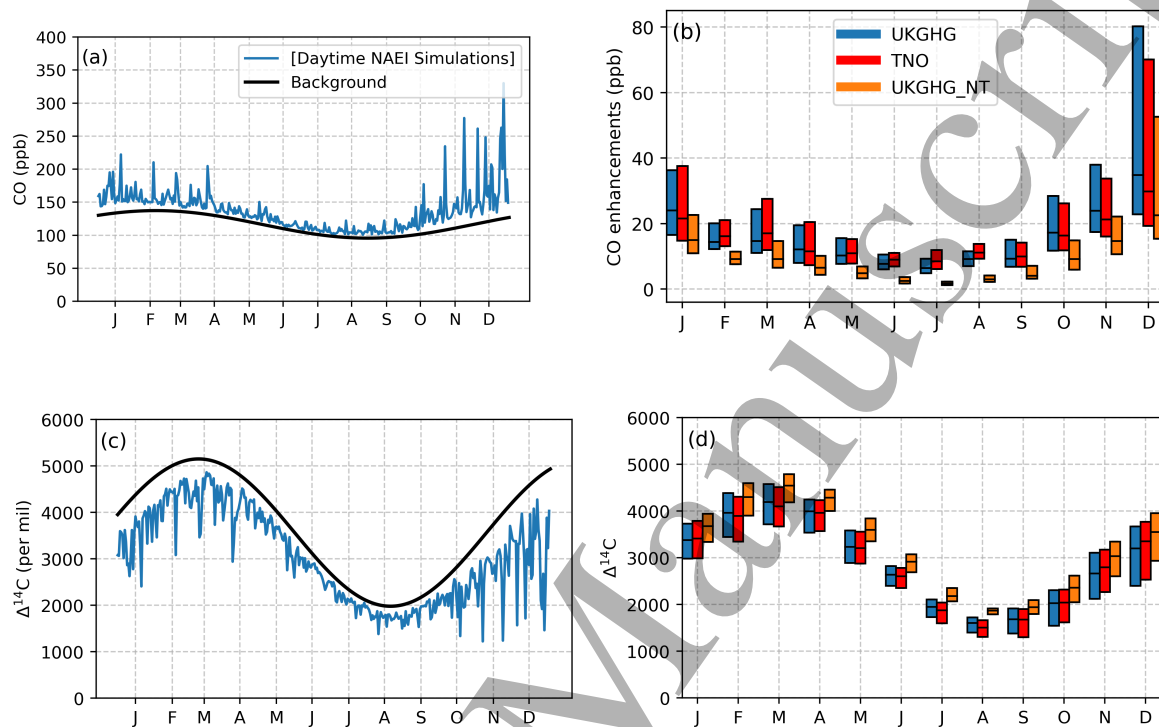


Figure 3: (a) Simulated CO enhancements at Imperial College London added to background CO concentrations from Mace Head, shown for afternoon hours (12:00 - 17:00 mean) in 2018 using UKGHG emissions. (b) Boxplots showing the 25th percentile, the median, and the 75th percentile of simulated CO enhancements for each month in 2018 from the three different emissions estimates. (c) Simulated  $\Delta^{14}\text{C}$  at Imperial College London with estimated background for afternoon hours (1200-1700 mean) in 2018 using UKGHG emissions. (d) Boxplots showing the 25th percentile, the median, and the 75th percentile of simulated  $\Delta^{14}\text{C}$  for each month in 2018 from the three different emissions estimates.

The average daily CO enhancements for simulations with UKGHG and TNO emissions are nearly the same in their yearly median values (13.97 ppb vs 14.13 ppb), however, there are differences in medians for some months (Figure 3b). CO enhancements from UKGHG\_NT are lower (yearly median: 9.8ppb), as expected since traffic emissions that comprise 44% of UKGHG emissions were removed. This is more apparent in the summer when traffic emissions dominate the overall budget.

The difference between  $\Delta^{14}\text{C}_m$  and  $\Delta^{14}\text{C}_{bg}$  ( $\Delta^{14}\text{C}_m - \Delta^{14}\text{C}_{bg}$ , hereinafter referred to as  $\Delta\Delta^{14}\text{C}$ ) varies with excess CO for the different simulations due to differences in fossil fraction (FF). Figure 4 shows the relationship between excess CO ( $\sum_i C_i$ ) and  $\Delta\Delta^{14}\text{C}$  for March and September in the simulations, and when the additional CO is purely fossil (-1000 ‰) or purely

## Radiocarbon as a Tracer of the Fossil Fraction of Regional Carbon Monoxide Emissions 10

biogenic (assuming 100 ‰). We chose these two months as they represent a large range of possible CO situations, one where background,  $\Delta^{14}\text{C}$  and CO emissions are high (March), and one where all of these quantities are low (September). These curves use the monthly average  $^{14}\text{C}$  as the background, and vary month by month due to the variation in the background  $\Delta^{14}\text{C}$  of CO, which affects the sensitivity of  $\Delta^{14}\text{C}$  to CO of different  $\Delta^{14}\text{C}$  signatures. The difference between background  $\Delta^{14}\text{C}$  in CO and fossil  $\Delta^{14}\text{C}$  doubles between August and March. Background  $\Delta^{14}\text{C}$  is also influenced by the solar cycle on multi-year timescales.

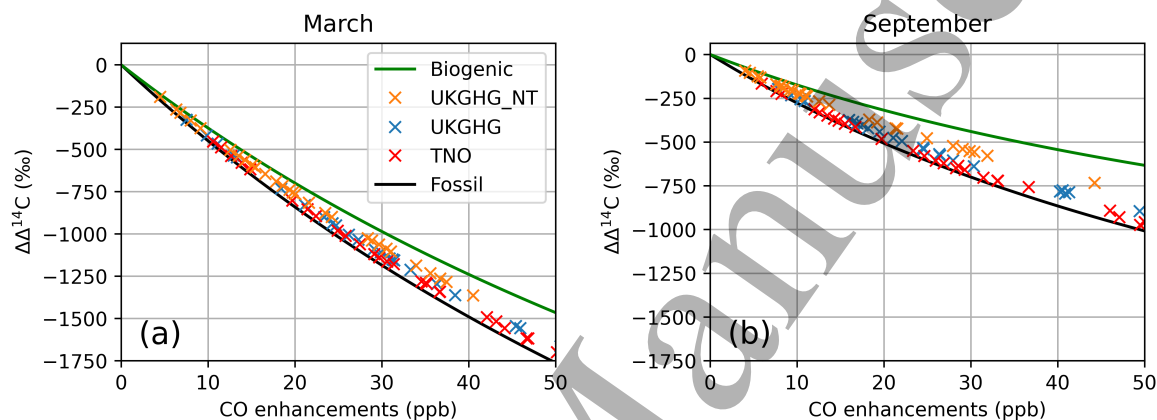


Figure 4: Simulated relationship between CO enhancements and  $\Delta\Delta^{14}\text{C}$  (daily mean) over two months (a) March and (b) September. All three emission schemes are shown, as well as ideal scenarios of purely fossil (black) and biogenic ( $\Delta^{14}\text{C} = 30$  ‰) (green) CO emissions.

The three emissions scenarios follow distinct curves in Figure 4 reflecting their different fossil fractions (Table 1). UKGHG\_NT has the lowest fossil fraction (yearly mean: 34%) and is nearest to the pure biogenic curve, while TNO has the highest fossil fraction (66%) and is nearest to the pure fossil curve. The UKGHG and TNO curves are closer to the pure fossil curve in summer months, when domestic combustion emissions are lower (Figure 2).

There is some scatter in the  $\Delta^{14}\text{C}$ -CO relationships for each scenario in Figure 4, reflecting spatio-temporal variations in excess CO and the fossil fraction of CO in London. As an example of how  $\Delta^{14}\text{C}$  and CO measurements could be interpreted for the monthly mean fossil fraction in excess CO, we compute idealized curves with different fossil fractions and find the best fit to the simulated data for each scenario. This best-fit fossil fractions can be seen in Figure 5, with error bars representing  $1\sigma$  uncertainties around the best-fit FF.

There is a lower fossil fraction in the winter than in the summer for UKGHG and TNO due to the increased domestic combustion emissions that use more biogenic fuel (Figure 2a). In contrast, in summer, the bulk of emissions arise from transport, nearly all from fossil fuels. The fossil fraction in UKGHG\_NT emissions remains relatively flat for the year, as the CO emissions in this regime are dominated by domestic combustion at all times with a fossil fraction of 34% (Table 1).

## Radiocarbon as a Tracer of the Fossil Fraction of Regional Carbon Monoxide Emissions 11

There are significant differences between the derived fossil fractions for the different emission scenarios, compared to the uncertainty in the fits ( $\approx 5\%$ ), indicating  $\Delta^{14}\text{C}$  measurements would help to refine CO source attribution in London. Uncertainties in  $\Delta^{14}\text{C}$  and CO measurement are comparable to the scatter in each scenario in Figure 4, suggesting that the uncertainties in derived fossil fraction would not be much larger than these estimated uncertainties. Considering the UKGHG\_NT scenario, it appears that  $\Delta^{14}\text{C}$  measurements would be able to track reductions in fossil fraction as the UK transitions to electric vehicles following bans on the sale of internal combustion and hybrid vehicles planned over the coming decade.

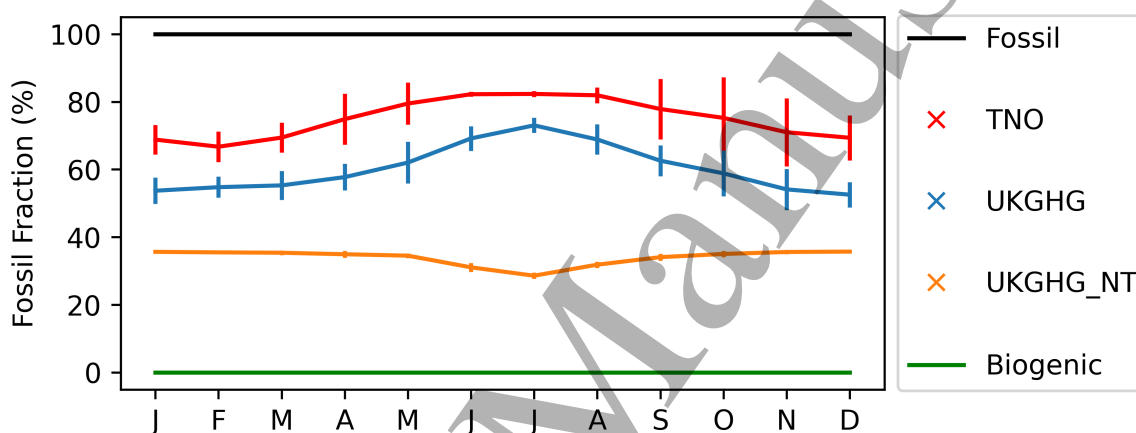


Figure 5: Derived mean monthly fossil fraction of CO at Imperial College London based on fitting simulated data from different emission schemes. Error bars show uncertainty in fits to idealised curves.

### 4. Potential methodology for exploiting $^{14}\text{C}$ CO measurements to determine CO fossil fraction

The results of our simulations using different emissions schemes and the NAME model demonstrate a proof of concept to understand how  $^{14}\text{C}$  CO measurements could be applied to determine the fossil fraction of CO at Imperial College or at other locations. To apply this technique, the required measured parameters are:

- Measurements of CO mixing ratio ( $C_m$ ) and  $\Delta^{14}\text{C}$  ( $\Delta_m$ ) at a measurement site
- Measurements of CO mixing ratio ( $C_{bg}$ ) and  $\Delta^{14}\text{C}$  ( $\Delta_{bg}$ ) at a background location
- Measurement or estimation of  $\Delta^{14}\text{C}$  of the biogenic source of CO in the region ( $\Delta_{bio}$ )

These data could then be plotted as in Figure 4, with  $\Delta\Delta^{14}\text{C}$  vs CO enhancements, and compared to idealised curves to find the average fossil fraction that best matches the data.

Alternatively, the fossil-derived CO ( $C_{ff}$ ) can be calculated directly from an individual measurement following the mass balances from Equations 1 and 2 using the equation (Turnbull

## Radiocarbon as a Tracer of the Fossil Fraction of Regional Carbon Monoxide Emissions 12

et al., 2006):

$$C_{ff} = \frac{(\Delta_m - \Delta_{bio})C_m - (\Delta_{bg} - \Delta_{bio})C_{bg}}{(\Delta_{ff} - \Delta_{bio})} \quad (4)$$

And the fossil fraction of the CO enhancement can be calculated using the equation:

$$FF = C_{ff}/(C_m - C_{bg}) \quad (5)$$

By propagating errors (see supplementary material), we find the uncertainty on measured  $C_{ff}$  would be  $\sim 10\%$  on an individual measurement for typical scenarios at Imperial College. This assumes the uncertainty of CO mixing ratio is  $\pm 2$  ppb, uncertainty of  $\Delta_{bio}$  is  $\pm 250\%$  and uncertainty of  $\Delta^{14}\text{CO}$  measurements to be  $\pm 125\%$  (Petrenko et al., 2021). Since the uncertainty in fossil fraction will be dominated by the uncertainty on the derived  $C_{ff}$ , uncertainty on calculated FF will also be  $\pm 10\%$ , which should allow us to trace a wide range of possible CO emissions scenarios. For other locations where CO enhancements are much higher, the uncertainty would be lower.

Some applications should also consider chemical sources, such as the oxidation of  $\text{CH}_4$  or VOCs (Dasari et al., 2021), or sinks from CO oxidation, which we neglected. One way of accounting for chemical effects might be to combine  $\Delta^{14}\text{C}$  with stable isotopic measurements of CO to enhance our understanding of the origin of excess CO.

### 5. Discussion and Conclusions

We presented the first regional-scale simulations of  $^{14}\text{CO}$  and showed that there are differences in  $\Delta\Delta^{14}\text{C}$ -excess CO relationships at Imperial College London driven by differences in the fossil fraction of CO emissions that should be detectable with current measurement precision. The capability of  $^{14}\text{CO}$  measurements to identify fossil fraction is unique, as  $^{13}\text{C}/^{12}\text{C}$  in CO from fossil fuels and biomass burning are similar (Vimont et al., 2017).

Our results indicate that  $^{14}\text{CO}$  measurements could be used to evaluate the fossil fraction of regional CO emissions and compared with bottom-up emission inventories, and to track trends in the fossil fraction of CO emissions over time. Evaluating and improving the source attribution of CO emissions would help to mitigate emissions and evaluate the effectiveness of mitigation policies, including the phaseout of internal combustion engines in the UK. Observations of seasonal changes in the fossil fraction of CO sources could also help to better understand CO sources.

A better understanding of CO sources could also benefit applications using CO measurements as a tracer for fossil fuel-derived  $\text{CO}_2$  (Turnbull et al., 2015). The use of CO as a tracer of fossil fuel-derived  $\text{CO}_2$  assumes that fossil fuel combustion is the dominant source of CO in a region, an assumption that could be checked with measurements of  $\Delta^{14}\text{C}$  in CO.

The sensitivity of  $\Delta^{14}\text{C}$  to regional emissions will change year on year because the background  $\Delta^{14}\text{CO}$  changes due to the solar cycle. For 2018, our background varies between 1978‰ and

## REFERENCES

13

5150‰, however, for a year with low solar activity we would expect this to be higher ( $\approx 2800$  -  $5550$  ‰), whilst in years with high solar activity, this would be lower ( $\approx 1100$  -  $2250$  ‰). Therefore, the sensitivity will be highest during solar minimum.

The application of  $\Delta^{14}\text{C}$  measurements to attribute CO sources may be particularly useful in the regions where CO sources may be less well-known. Considering global emissions of CO (shown for two bottom-up estimates in Figure 1), the highest emissions of CO in 2014 are in Asia and Africa, which also have the largest differences between bottom-up estimates and are among the places with the strongest growth in emissions since 1980. The technique would also be more effective there due to the stronger sources of CO and higher excess CO concentrations. In addition, there is less variation in  $\Delta^{14}\text{C}$  of background CO in lower latitudes compared to higher latitudes, which could reduce the uncertainty in the derived fossil fraction.

## 6. Acknowledgments

L. B. was supported by the Grantham Institute—Climate Change and the Environment and the Natural Environment Research Council [NE/S007415/1]. H. G. would like to acknowledge funding from the Natural Environment Research Council [NE/X001040/1], from a Royal Society Wolfson Fellowship [RSWF/FT/191013] and from Schmidt Sciences through the Fate, Emissions, and Transport of  $\text{CH}_4$  (FETCH4) project. Analysis code was based on functions provided by Dr Hannah Chawner (previously of University of Bristol).

## 7. Data Availability

NAEI mapped emissions for 2018 can be found at: <https://naei.beis.gov.uk/data/mapping-archive> whilst UKGHG time variations can be applied using R package at <https://github.com/NERC-CEH/ukghg>. Total yearly emissions allocated by fuel source can be found at: <https://naei.beis.gov.uk/data/data-selector>.

TNO\_CAMSv5.3 are available to download directly from ECCAD website (<https://eccad.aeris-data.fr>). CAMS\_TEMPO, the temporal variability applied to TNO\_CAMSv5.3 emissions can be found at: <https://eccad.sedoo.fr/#/metadata/506> (last accessed November 2023)

Estimated background CO and  $\Delta^{14}\text{C}$ , along with simulated CO and  $\Delta^{14}\text{CO}$  for each emission scheme can be found in supplemental data in Table S2. The mapping between NFR and SNAP sectors is found in supplemental data in Table S1. The SNAP sector emissions, split into fuel sources, can be found in supplemental data in Table S3.

## References

Al-Naiema, Ibrahim M., Subin Yoon, Yu Qin Wang, Yuan Xun Zhang, Rebecca J. Sheesley and Elizabeth A. Stone (2018). "Source apportionment of fine particulate matter organic carbon in Shenzhen, China by chemical mass balance and radiocarbon methods". In: *Environmental Pollution* 240, pp. 34–43. ISSN: 18736424. DOI: 10.1016/j.envpol.2018.04.071.

## REFERENCES

14

- Andersen, Christopher, Matthias Ketzel, Ole Hertel, Jesper H. Christensen and Jørgen Brandt (2024). “The Danish Lagrangian Model (DALM): Development of a new local-scale high-resolution air pollution model”. In: *Environmental Modelling & Software* 176. ISSN: 1364-8152. DOI: 10.1016/j.envsoft.2024.106010.
- Brenninkmeijer, Sergey S. C. A. M. Gromov and Patrick Jöckel (2022). “Cosmogenic <sup>14</sup>C for assessing the OH-based self-cleaning capacity of the troposphere”. en. In: *Radiocarbon* 64.4, pp. 761–779. DOI: 10.1017/RDC.2021.101.
- Dasari, Sanjeev, August Andersson, Maria E Popa, Thomas Röckmann, Henry Holmstrand, Krishnakant Budhavant and O Rjan Gustafsson (2021). “Observational Evidence of Large Contribution from Primary Sources for Carbon Monoxide in the South Asian Outflow”. In: *Cite This: Environ. Sci. Technol* 2022, pp. 165–174. DOI: 10.1021/acs.est.1c05486.
- Derwent, Richard G., David D. Parrish, Peter G. Simmonds, Simon J. O’Doherty and T. Gerard Spain (2020). “Seasonal cycles in baseline mixing ratios of a large number of trace gases at the Mace Head, Ireland atmospheric research station”. In: *Atmospheric Environment* 233, p. 117531. ISSN: 1352-2310. DOI: 10.1016/j.atmosenv.2020.117531.
- Ding, Aijun, Tao Wang and Congbin Fu (2013). “Transport characteristics and origins of carbon monoxide and ozone in Hong Kong, South China”. en. In: *Journal of Geophysical Research: Atmospheres* 118.16, pp. 9475–9488. ISSN: 2169-8996. DOI: 10.1002/jgrd.50714.
- Duncan, Bryan N., J. A. Logan, I. Bey, I. A. Megretskaya, R. M. Yantosca, Paul C. Novelli, N. B. Jones and C. P. Rinsland (2007). “Global budget of CO, 1988 - 1997: Source estimates and validation with a global model”. In: *Journal of Geophysical Research Atmospheres* 112.22, pp. 1988–1997. ISSN: 01480227. DOI: 10.1029/2007JD008459.
- Elguindi, N. et al. (2020). “Intercomparison of Magnitudes and Trends in Anthropogenic Surface Emissions From Bottom-Up Inventories, Top-Down Estimates, and Emission Scenarios”. In: *Earth’s Future* 8.8, pp. 1–20. DOI: 10.1029/2020EF001520.
- Graven, H et al. (2018). “Assessing fossil fuel CO<sub>2</sub> emissions in California using atmospheric observations and models”. In: *Environmental Research Letters* 13.6. DOI: 10.1088/1748-9326/aabd43.
- Graven, Heather et al. (2017). “Compiled records of carbon isotopes in atmospheric CO<sub>2</sub> for historical simulations in CMIP6”. English. In: *Geoscientific Model Development* 10.12, pp. 4405–4417. ISSN: 1991-959X. DOI: 10.5194/gmd-10-4405-2017.
- Guevara, Marc, Oriol Jorba, Carles Tena, Hugo Denier Van Der Gon, Jeroen Kuenen, Nellie Elguindi, Sabine Darras, Claire Granier and Carlos Pérez García-Pando (2021). “Copernicus Atmosphere Monitoring Service TEMPORal profiles (CAMS-TEMPO): global and European emission temporal profile maps for atmospheric chemistry modelling”. In: *Earth Syst. Sci. Data* 13, pp. 367–404. DOI: 10.5194/essd-13-367-2021.
- Hernández-Paniagua, Iván Y. et al. (2018). “Diurnal, seasonal, and annual trends in tropospheric CO in Southwest London during 2000–2015: Wind sector analysis and comparisons with urban and remote sites”. In: *Atmospheric Environment* 177, pp. 262–274. DOI: 10.1016/j.atmosenv.2018.01.027.

## REFERENCES

15

- Hoesly, Rachel M et al. (2018). “Historical (1750-2014) anthropogenic emissions of reactive gases and aerosols from the Community Emissions Data System (CEDS)”. In: *Geosci. Model Dev* 11, pp. 369–408. DOI: 10.5194/gmd-11-369-2018.
- Holloway, Tracey, Hiram Levy II and Prasad Kasibhatla (2000). “Global distribution of carbon monoxide”. en. In: *Journal of Geophysical Research: Atmospheres* 105.D10, pp. 12123–12147. DOI: 10.1029/1999JD901173.
- Jöckel, Patrick and Carl A. M. Brenninkmeijer (2002a). “The seasonal cycle of cosmogenic  $^{14}\text{C}$  at the surface level: A solar cycle adjusted, zonal-average climatology based on observations”. en. In: *Journal of Geophysical Research: Atmospheres* 107.D22, ACH 23–1–ACH 23–20. DOI: 10.1029/2001JD001104.
- Jöckel, Patrick, Carl A M Brenninkmeijer, Mark G Lawrence, Adriaan B M Jeuken, Peter F J van Velthoven, A M Brenninkmeijer, M G Lawrence, A B M Jeuken and P F J van Velthoven (2002b). “Evaluation of stratosphere-troposphere exchange and the hydroxyl radical distribution in three-dimensional global atmospheric models using observations of cosmogenic  $^{14}\text{C}$ ”. In: *J. Geophys. Res* 107.20, p. 4446. DOI: 10.1029/2001JD001324.
- Klouda, G A, L A Currie, D J Donahue, A J T Jull and M H Naylor (1986). “Urban Atmospheric  $^{14}\text{C}$  CO and  $^{14}\text{C}$  CH<sub>4</sub> Measurements by Accelerator Mass Spectrometry”. en. In: *Radiocarbon* 28.2A, pp. 625–633. DOI: 10.1017/S0033822200007815.
- Klouda, George A. and Michael V. Connolly (1995). “Radiocarbon ( $^{14}\text{C}$ ) measurements to quantify sources of atmospheric carbon monoxide in urban air”. In: *Atmospheric Environment* 29.22, pp. 3309–3318. DOI: 10.1016/1352-2310(95)00223-L.
- Kunz, C. (1985). “Carbon-14 Discharge at Three Light-water Reactors”. en-US. In: *Health Physics* 49.1, p. 25. ISSN: 0017-9078.
- Lelieveld, Jos, Sergey Gromov, Andrea Pozzer and Domenico Taraborrelli (2016). “Global tropospheric hydroxyl distribution, budget and reactivity”. In: *Atmos. Chem. Phys* 16, pp. 12477–12493. DOI: 10.5194/acp-16-12477-2016.
- Lowry, D et al. (2016). “Marked long-term decline in ambient CO mixing ratio in SE England, 1997-2014: Evidence of policy success in improving air quality”. In: *Scientific Reports* 6. DOI: 10.1038/srep25661.
- Moriizumi, Jun, Akihiko Goto and Takao Iida (2004). “A new extraction technique for atmospheric  $^{14}\text{C}$  and its application”. In: *Nuclear Instruments and Methods in Physics Research Section B: Beam Interactions with Materials and Atoms*. Proceedings of the Ninth International Conference on Accelerator Mass Spectrometry 223-224, pp. 511–515. DOI: 10.1016/j.nimb.2004.04.096.
- Petrenko, Vasilii V, Andrew M Smith, Edward M Crosier, Roxana Kazemi, Philip Place, Aidan Colton, Bin Yang, Quan Hua and Lee T Murray (2021). “An improved method for atmospheric  $^{14}\text{C}$  CO measurements”. In: *Atmos. Meas. Tech* 14. DOI: 10.5194/amt-14-2055-2021.
- Poluianov, S. V., G. A. Kovaltsov, A. L. Mishev and I. G. Usoskin (2016). “Production of cosmogenic isotopes  $^7\text{Be}$ ,  $^{10}\text{Be}$ ,  $^{14}\text{C}$ ,  $^{22}\text{Na}$ , and  $^{36}\text{Cl}$  in the atmosphere: Altitudinal profiles of yield functions”. In: *Journal of Geophysical Research: Atmospheres* 121.13, pp. 8125–8136. DOI: 10.1002/2016JD025034.



## REFERENCES

16

- Quay, Paul, Stagg King, David White, Melinda Brockington, Beth Plotkin, Richard Gammon, Steven Gerst and John Stutsman (2000). “Atmospheric  $^{14}\text{CO}$ : A tracer of OH concentration and mixing rates”. en. In: *Journal of Geophysical Research: Atmospheres* 105.D12, pp. 15147–15166. DOI: 10.1029/2000JD900122.
- Saboya, Eric, Giulia Zazzeri, Heather Graven, Alistair J Manning and Sylvia Englund Michel (2022). “Continuous  $\text{CH}_4$  and  $^{13}\text{CH}_4$  measurements in London demonstrate under-reported natural gas leakage”. In: *Atmospheric Chemistry and Physics* 22.5, pp. 3595–3613. DOI: 10.5194/acp-22-3595-2022.
- Sakugawa, Hiroshi and Isaac R Kaplan (1997). *Radio and stable-isotope measurements of atmospheric carbon monoxide in Los Angeles\**. Tech. rep., p. 75.
- Shindell, D et al. (2013). “Anthropogenic and Natural Radiative Forcing. In: Climate Change 2013: The Physical Science Basis. Contribution of Working Group I”. In.
- Sinha, Ashok and Ralf Toumi (1996). “A Comparison of Climate Forcings Due to Chlorofluorocarbons and Carbon Monoxide”. In: *Geophysical Research Letters* 23.1, pp. 65–68. ISSN: 1944-8007. DOI: 10.1029/95GL03593.
- Stuiver, Minze and Henry A. Polach (1977). “Reporting of  $^{14}\text{C}$  data”. In: *Radiocarbon* 19.3. ISBN: 0033-8222, pp. 355–363. ISSN: 1872-6283.
- Turnbull, J. C., J. B. Miller, S. J. Lehman, P. P. Tans, R. J. Sparks and J. Southon (2006). “Comparison of  $^{14}\text{CO}_2$ , CO, and  $\text{SF}_6$  as tracers for recently added fossil fuel  $\text{CO}_2$  in the atmosphere and implications for biological  $\text{CO}_2$  exchange”. en. In: *Geophysical Research Letters* 33.1. DOI: 10.1029/2005GL024213.
- Turnbull, Jocelyn C. et al. (2015). “Toward quantification and source sector identification of fossil fuel  $\text{CO}_2$  emissions from an urban area: Results from the INFLUX experiment”. In: *Journal of Geophysical Research* 120.1, pp. 292–312. DOI: 10.1002/2014JD022555.
- Vimont, Isaac J. et al. (2017). “Carbon monoxide isotopic measurements in Indianapolis constrain urban source isotopic signatures and support mobile fossil fuel emissions as the dominant wintertime CO source”. In: *Elementa* 5, pp. 1–17. DOI: 10.1525/elementa.136.
- Zheng, Bo, Frederic Chevallier, Philippe Ciais, Yi Yin, Merritt N. Deeter, Helen M. Worden, Yilong Wang, Qiang Zhang and Kebin He (2018). “Rapid decline in carbon monoxide emissions and export from East Asia between years 2005 and 2016”. In: *Environmental Research Letters* 13.4. DOI: 10.1088/1748-9326/aab2b3.